Available online at www.sciencedirect.com
SCIENCE DIRECT®
Polymer 45 (2004) 2911–2920
polymer
www.elsevier.com/locate/polymer

A modified model predictions and experimental results of weld-line strength in injection molded PS/PMMA blends

Shaoyun Guo[a,*], A. Ait-Kadi[b], M. Bousmina[b]

[a]*The State Key Laboratory of Polymer Materials Engineering, Polymer Research Institute, Sichuan University, Chengdu, 610065, China*
[b]*CERSIM, Department of Chemical Engineering, Laval University, Laval, Que., Canada G1K 7P4*

Received 9 October 2003; received in revised form 11 February 2004; accepted 23 February 2004

Abstract

In this paper, the model based on melt diffusion and Flory–Huggins free energy theory for predicting the weld-line strength of injection molded amorphous polymers and polymer blends parts were modified by considering the diffusion thickness in the interface as a function of contact time. The modified model for weld-line strength prediction of homopolymers and polymer blends were, respectively, used to evaluate the weld-line strength of Polystyrene (PS) and Poly(methylmethacrylate) (PMMA), and that of PS/PMMA blends. The model predictions show that the theoretic predictions as a function of temperature and contact time for PS, PMMA and PS/PMMA (80/20, 70/30) are in good agreements with corresponding experimental results. However, the model predictions for PS/PMMA (20/80, 30/70) blends are much higher than experimental results. The morphology in weld-line regions for PS/PMMA (20/80, 30/70) shows lack of dispersed PS phase. Near the weld-line regions, dispersed PS phase is highly oriented along the weld-line. In theoretic prediction for polymer blends, three kinds of diffusion: Polymer A–Polymer A and Polymer B–Polymer B self-diffusions and Polymer A–Polymer B mutual diffusion were considered. This is why model predictions for PS/PMMA (20/80, 30/70) blends are higher than experimental results.

Keywords: PS; PMMA; Blends

1. Introduction

The injection molding is one of the most attractive polymer processes in industry. It is especially used to produce a wide variety of complex geometry articles (e.g. precision gear wheel, hampers… etc.) in a single operation and low wear of the processing equipment. High production rate, short cycle times and low percentage of scrap are also accounting the advantages that make. This process is very attractive from engineering and economical point of view. However, molding complicated parts, multi-gated mold cavities and cavities containing inserts may generate serious difficulties in terms of mold filling and final production especially. In fact, molding of such parts usually produces weld-line once the melt fronts have joined either by impingement flow or around an insert [1,2]. Weld-lines also form when jetting occurs along the flow path where the flow is suddenly accelerated (e.g. near the gate) [3]. Although the weld-lines are formed as the mold is being filled, their structure, shapes, and properties are affected by the entire injection molding cycle. It is well known that the weld-line is a potential source of weakness. The weld-line structure and properties are mainly due to [4–6]:

- orientation of molecules along the weld-line rather than across it as a result of deformation of polymer after the two polymer melt fronts collide;
- partial cooling of the melt front at the interface leading to skin formation and
- formation of a relatively sharp V-notch at the weld-line caused by the entrapped air which is forced to the wall.

In unfilled amorphous polymers the properties of a weld-line will depend on whether the polymer chains had enough time to diffuse across the interface to form a strong bond [7]. The weakness of the weld-line is attributed to the incomplete bonding at the interface, to the molecular orientation parallel to the interface and to the existence of V-notches at the surface around the weld-line [7]. Kim and

* Corresponding author. Tel.: +86-288-540-5135; fax: +86-288-540-2465.
E-mail address: nic7702@scu.edu.cn (S. Guo).

0032-3861/$ - see front matter © 2004 Elsevier Ltd. All rights reserved.
doi:10.1016/j.polymer.2004.02.051

Suh [8] presented a model for the strength of the weld-line based on the self-diffusion of molecular chains across the polymer–polymer interface and on the molecular orientations parallel to the weld-line plan generated at the melt front. Their results are presented in terms of melt temperature for a given contact time. Model prediction and experimental results are found to compare fairly well.

A number of studies have focused on the effects of processing parameters like melt temperature, holding pressure, holding time, injection velocity and mold temperature on weld-line structure and properties of thermoplastics [4,8–22]. The results showed that weld-line strength could be greatly improved by selection of suitable injection molding processing parameters. Melt temperature, injection velocity, holding pressure, holding time and mold temperature will all affect weld-line strength to various degrees depending on materials. In general, high melt temperature, high hold pressure and high mold temperature can produce high weld-line strength. The melt temperature is the most important parameter for influencing weld-line strength. It is obvious that the processing parameters beneficial to molecular diffusion across weld-line can improve weld-line strength. Other innovative techniques such as tooling modification [23], multi-live feed injection molding process [24], an asymmetric packing flow produced by proper design of the two gates [25] and shear controlled orientation in injection molding (Scorim) for improvement of weld-line strength were also investigated [26]. Besides processing parameters, weld-line strength also greatly replies on the properties of materials [14,27–29]. For unfilled polymers, the lowest weld-line strength was obtained for brittle amorphous polymers and rod-like polymers like PS, PMMA, SAN, LCP, Acetal etc., higher values are usually obtained for ductile amorphous or crystalline polymers such as PP, PE, PBT, PET, PVC and PC. Using PMMA having different molecular weight, Mening [30] found that the weld-line strength decreases with increasing molecular weight. His results are in agreement with the self-diffusing approach of Kim and Suh [8].

The V-notch formation in amorphous polymers is attributed to a viscosity increase in the outermost layer of molding. The particular problem can be partially overcome by adequately placing vent in the weld-line area [31]. The trapped air may also cause local heating and polymer degradation thereby contributing weld-line weakness [32].

For semi-crystalline polymers, the situation is even more complicated. Indeed, in addition to the above mentioned parameters, the degree of crystallinity, the size and the distribution of the crystallites in the weld-line region have also important effects on the weld-line strength [33–35]. The effect of processing parameters (mold and melt temperatures, cooling rate, and injection pressure) is however found to be similar to the observed for their amorphous counterpart [10,11,36–38]. The more pronounced shrinkage of the semi-crystalline polymers as compared to amorphous ones is found to have an important effect on the V-notch which forms a sharp ridge upon cooling [39,40]. The presence of inhomogeneities (abraded particles, impurities, mold release agent) is also found to affect weld-line strength through nucleation of crystallites [39,40]. Mielewski et al. [41] identified the cause of weld-line weakness in polypropylene systems containing a hindered phenolic antioxidant additive. A combination of techniques, TEM, Izod impact strength and tensile strength measurements and XPS confirmed that a major cause of weakness in polypropylene weld-lines was the accumulation of a heat stabilizer additive on the flow front tip and the surface of the part. In the case of immiscible polymer blends weld-lines are found to be much weaker than for homopolymers [42–44]. The situation is even more complicated by the presence of preformed structural differences and minor phase concentration gradients in the weld region [45–48]. Using compatibilizers to stabilize and reduce minor phase dimensions is found to increase weld strength [44,49]. The presence of compatibilizer is also found to narrow the weld-line region. In all cases, failure occurs at the weld-line. Welded samples are found here also to be very sensitive to processing conditions [50–52]. Increasing mold temperature and injection temperature for example help restore the strength loss but never to the point where the strength reaches that of the unwelded samples [43].

Attempts to quantify the weld-line strength have been presented. Models based on molecular diffusion have been used for homopolymers [8,53,54] and for immiscible polymer blends [43]. Kim and Suh [8] assumed that the entire load is 'beard' by the bounded area of the specimen. This idea is expressed in the following equation [8]:

$$\sigma_w = \sigma_b\left(\frac{A_0 - A_N}{A_0}\right) \tag{1}$$

where σ_w and σ_b are the tensile strength of the injection molded part with and without weld-line, respectively, A_0 is the initial cross-sectional area of the interface, A_N is the non-bonded area, and $A_0 - A_N$ is the bonded area at specific contact time.

They [8] further supposed that the time variation rate of the non-bounded area is given by Fick's Law of diffusion:

$$\frac{dA_N}{dt} = C\frac{D\Delta G}{kT} \tag{2}$$

where C is the constant, D is diffusion coefficient, and k is the Boltzmann constant, T is the absolute temperature, ΔG is the free-energy difference, and written as:

$$\Delta G = -2\gamma A_N - T\Delta S_m \tag{3}$$

where γ is the surface tension, and ΔS_m is the entropy of mixing determined from the Flory–Huggins theory of lattice [62].

With an expression of the entropy of mixing given by the Flory–Huggins lattice theory they obtained an expression of

the new bounded area as a function of the contact time and other parameters appearing in Eq. (1)–(3). Detailed calculations will be given in a coming section. From Eq. (1) they then obtained an expression for σ_w as a function of the same set of parameters. Hamada et al. [54] proposed a useful parameter, weld-line index ϕ to estimate weld-line property of injection molding.

$$\phi = \int_{-h}^{h} \int_{t} \frac{\partial t}{\tau} \partial y \tag{4}$$

where 2 h is thickness, t is time, τ is viscoelastic relaxation time of polymer melt which was measured using cone plate type rheometer. The relationship of τ with mechanical property of injection moldings with a weld-line was discussed for PS and PC. Polymer melt whose τ was relatively short can easily enhance the entanglement across the weld-line interface and weld-line strength. Polymers, which have large weld-line index basically, tend to have high weld-line strength. Weld-line index itself considers not only material property, but also molding conditions such as temperature, pressure etc.

Pecorini and Seo [53] assume that sufficient interpenetrates has occurred when the chains have diffused one radius of gyration obtained the following equation for the healing time:

$$t_h = R_g^2/2D_s \tag{5}$$

where using the following equation for the self-diffusion coefficient D_s

$$D_s = \left(\frac{\rho RT}{270}\right)\left(\frac{M_c}{M}\right)^2\left(\frac{R_g^2}{M}\right)\left(\frac{1}{\eta_{M_c,T}}\right) \tag{6}$$

where ρ is the melt density, T is the processing temperature, R is the gas constant, M_c is the critical molecular weight, M is the absolute molecular weight, and $\eta_{M_c,T}$ is the zero-shear viscosity at the critical molecular weight and processing temperature. With a detailed rheological characterization, they obtained the healing time as a function of temperature. The theoretical results compared well to weld-line Izod experimental data. Mekhilef et al. [43] extended the approach of Kim and Suh [8] to the case of immiscible polymer blends. Contribution to the weld-line strength from AA and BB self-diffusion was taken into account using Kim and Suh [8] approach. While AB diffusion was also taken into account using an expression for the free energy comprising the entropy of mixing of two different components and a contribution of the free surface of each constituent. Details of the approach will be given in Section 4 of the present work. Comparison of model predictions with experimental results obtained with a polycarbonate (PC) and high-density polyethylene (HDPE) blends showed that the model predicts fairly well the experimental data for a concentration and temperature utilized. Discrepancy between model predictions and experimental data for certain composition was attributed to the fact that their approach, unlike the one of Kim and Suh [8], does not take into account molecular orientation which may take place at the flow front due to the so-called 'fountain flow', nor does take into account the effect of temperature gradients that might be generated during the non-isothermal filling. Their set of experimental results did not allow to explore a wide range of filling temperature and hence to study the effect of temperature on the weld-line strength. Indeed the processing condition required by their specific blend did not allow for a good evaluation of the effect of minor phase (HDPE) to the weld-line strength as the lowest injection temperature and the contact time used for their experiments always result in a coagulate healing of the HDPE phase.

In this study, weld-line strength results for immiscible blends of constituents having similar processing conditions will be presented. Experimental data for different compositions and processing conditions will first be shown and then compared to a modified Mekhilef et al. [43] model.

2. Experimental

2.1. Materials

The materials used in this study are PMMA (Plexiglas™ V052, MI = 2.8 g/10 min, $\rho = 1.19$ g/cm^3, $M_w = 55,700$) supplied by AtoHass and PS (polystyrene 101, MI = 2.2 g/10 min, $\rho = 1.04$ g/cm^3, $M_w = 295,000$) supplied by Novacor Plastics Division.

2.2. Blending

PMMA and PS were dried at 80 °C prior to blending for 5 h to remove all the moisture. PMMA and PS with different composition ratios (PS/PMMA: 80/20, 70/30, 30/70, 20/80 by weight) were blended in a Haake twin-screw extruder at a screw speed of 60 rpm and a temperature profile ranging from 160 °C near the hopper to 200 °C at the die exit. The extrudate was then continuously cooled in a water bath and then pelletized.

2.3. Injection molding

PS, PMMA and their blends were dried at 80 °C for 4 h prior to injection molding. All samples were prepared on a Nissel fully hydraulic 68 tons injection molding machine having a maximum injection capacity of 114 cm^3/shot. The molded contained two ASTM standard dogbone-shaped cavities for mechanical testing for both welded and non-welded specimens in this study is shown in Fig. 1. The specimen without a weld-line (here called 'NWL') and those with weld-line called 'WL'. Injection time is 10 s, cooling time is 25 s, injection temperatures are 180–260 °C, and mold temperature is 32 °C. Specimens with and without weld-line were prepared.

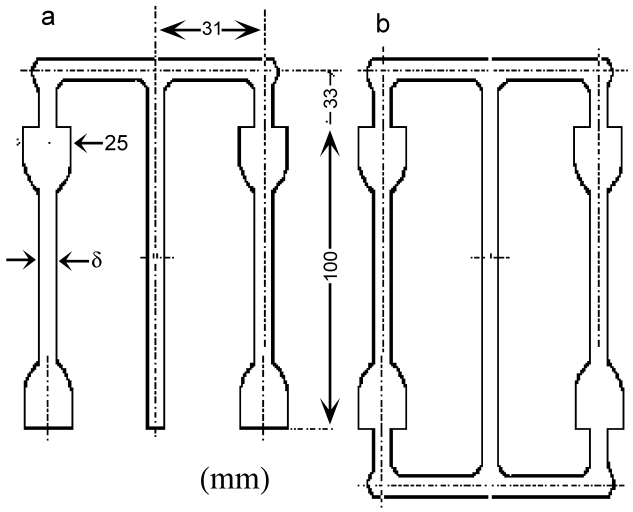

Fig. 1. Schematic diagram of mold cavity used for injection-molding samples with and without weld-line (a) no weld-line, (b) with weld-line.

2.4. Measurement and characterization

Tensile tests are made at room temperature using an Instron tensile testing machine at a cross-head speed of 5 mm/min at room temperature according to ASTM D638 standard method.

For rheological behavior, the samples were compression molded at 200 °C into 25 mm disks in diameter and ca. 1.5 mm in thickness. A Bohlin Rheometer CS was used to measure the dynamic viscoelastic properties of PS, PMMA and their blends with parallel plate geometry. Measurements were performed in the frequency range from 0.01 to 10 Hz at temperatures between 180 and 240 °C by steps of 20 °C. The measurements were done in a nitrogen atmosphere to avoid premature thermal degradation of the samples. Strain values were kept with the linear region. The zero viscosity (η_0) has been determined from cole–cole plots of η'' versus η'. The activation flow energy of PS, PMMA and their blends were calculated according to Arrhenius Equation $\eta_0 = A\, e^{(E_a/RT)}$, where A is a constant, E_a is the flow activation energy. Table 1 shows the zero shear viscosity and flow activation energy obtained from dynamic measurements.

3. Experimental results

During extrusion and injection molding processes, amorphous polymers properties exhibit significant variations throughout the thickness due to phenomena such as matrix orientation, residual stress, etc. which affect the tensile strength [55]. Orientation is always much more important in layers close to the surface than in the core [56]. Increasing melt temperature can significantly reduce the overall level of orientation in the molded part. It has shown that at high frequency, PS and PMMA show a power-law behavior. It is interesting to note that, in the low frequency region, the viscosity of PS is greatly influenced by the temperature, whereas a slight decrease is observed for PMMA, therefore, the tensile strength would be affected. Fig. 2 shows the tensile strength of homopolymers PS-NWL and PMMA-NWL as a function of the melt temperature. For PS-NWL, the tensile strength decreases dramatically with increasing melt temperature, while for PMMA-NWL, a slight decrease is recorded.

The effect of the weld-line on the morphology of both PS-WL and PMMA-WL specimens, was observed as straight line in the middle of cut samples. Fig. 3 shows the relationship between the melt temperature and the tensile strength of PS-WL and PMMA-WL. For both polymers, the weld-line strength increases with increasing the melt temperature. It was postulated that for PS-WL, the depth of weld-line is mainly related to the melt temperature [8,57]. It decreases with increasing the melt temperature. It is the time the polymer has to spend to diffuse across the interface, relative to relaxation or reentanglement time that appears to determine the weld-line strength.

In polymer blend, the viscosity ratio appears to be the dominant parameter in controlling the effect of melt temperature upon the tensile strength. However, when the viscosity of the matrix is lower than that of dispersed phase e.g. PS/PMMA-NWL, the viscosity ratio of PS/PMMA-NWL blend is relatively close to unity and decreases with melt temperature. Then, the matrix behavior (PS) got the better of dispersed phase (PMMA). Also, for the low interfacial tension found with PS/PMMA (1.5 mNm^{-1}), a very thin interfaces as well as an intimate contact is observed due to the presence of specific interaction. It was shown that PS/PMMA-NWL exhibits a droplet-matrix morphology for concentration of the minor phase (PS) as high as 35 vol% [58]. This might be attributed to the fact that a low interfacial tension prevents the phases from break up and coalescence. The tensile strength is found to be decreased with increasing melt temperature (Fig. 2). However, for PMMA/PS-NWL blend, it is surprising that

Table 1
Zero shear viscosities and flow activation energy of PS/PMMA blends

PS/PMMA		100/0	80/20	70/30	30/70	20/80	0/100
η_0 (Pa s)	180 °C	9.512×10^5	1.089×10^6	1.371×10^6	3.442×10^6	4.017×10^6	3.406×10^6
	200 °C	1.738×10^5	2.099×10^5	2.425×10^5	5.855×10^5	6.545×10^5	5.637×10^5
	220 °C	7.107×10^4	6.109×10^4	6.803×10^4	1.544×10^5	1.496×10^5	1.332×10^5
E_a (kJ/mol)		121.0	134.0	139.7	144.4	153.0	150.7

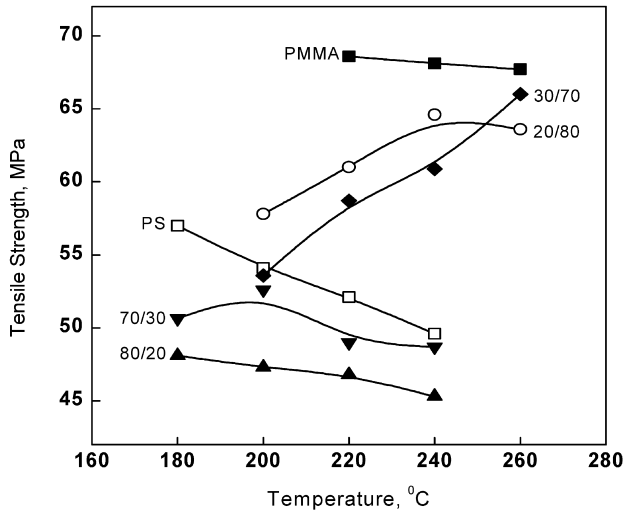

Fig. 2. Effect of injection temperature on tensile strength of PS/PMMA without weld-line.

despite the blending by PS, the PMMA matrix behavior is changed (Fig. 2). The morphology of PMMA/PS-NWL consists of tightly packed dispersed phase in matrix. This might indicate that coalescence of PS has not yet occurred. The tensile strength increases as the melt temperature increases. Otherwise, in addition to the viscosity ratio effect, the morphology, size and shape play a major role on controlling the blends behavior.

However, for PS/PMMA-WL, the weld-line strength increases with increasing the melt temperature. As shown in Fig. 3, the amplitude of the weld-line strength increase in PS/PMMA-WL blend is higher than that observed with PMMA/PS-WL. This means that the bonding and the V-notches formation at the interface seem to be important parameter on weld-line strength variation. Fig. 4 shows the effect of the PMMA content on the tensile strength of

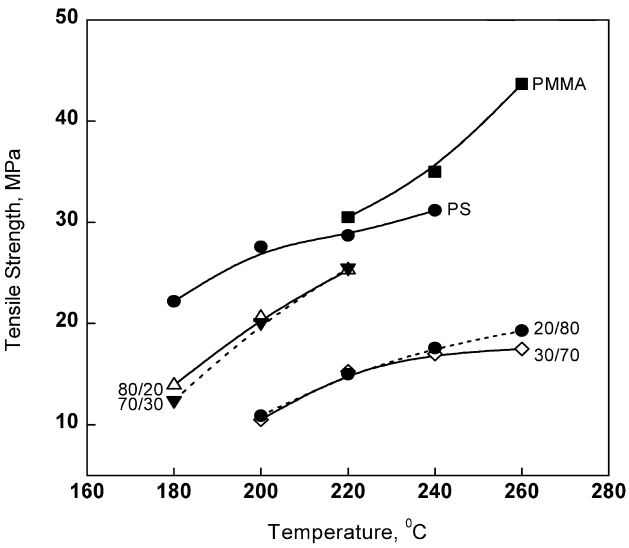

Fig. 3. Effect of injection temperature on tensile strength of PS/PMMA with weld-line.

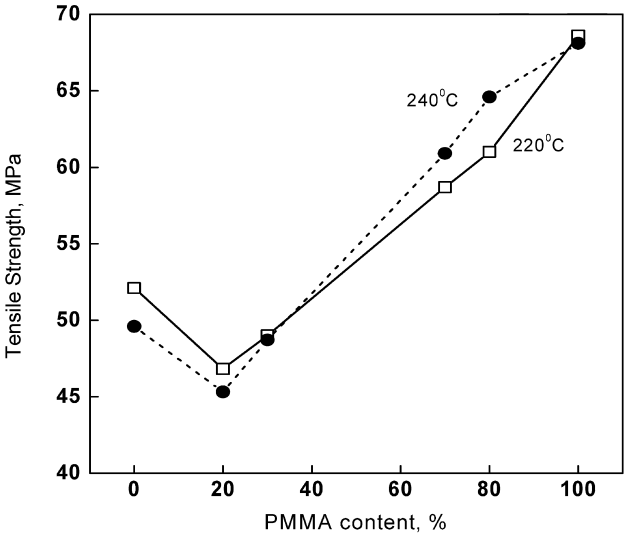

Fig. 4. Effect of PMMA content on tensile strength of PS/PMMA blends without weld-line.

PS/PMMA-NWL. The tensile strength increases with increasing PMMA content (Fig. 4). While the tensile strength of PS/PMMA-WL decreases with increasing PMMA content (Fig. 5). The volume content close to 80 vol% could be defined as a 'phase inversion point', since the weld-line increases.

Fig. 6 shows the SEM of cross and longitudinal sections of weld-line morphology for PMMA/PS-WL (70/30) blend (melt temperature 240 °C). On the longitudinal section, in addition to the V-notch formation, the weld-line appears to consist of escaped and/or deformed PS particles oriented parallel to the weld-line (Fig. 6a). But the dispersed PS phase is absent at the weld-line (Fig. 6b). At cross section, a rougher surface (500 μm) is observed at skin region, attributed to the dispersion PS phase accumulation.

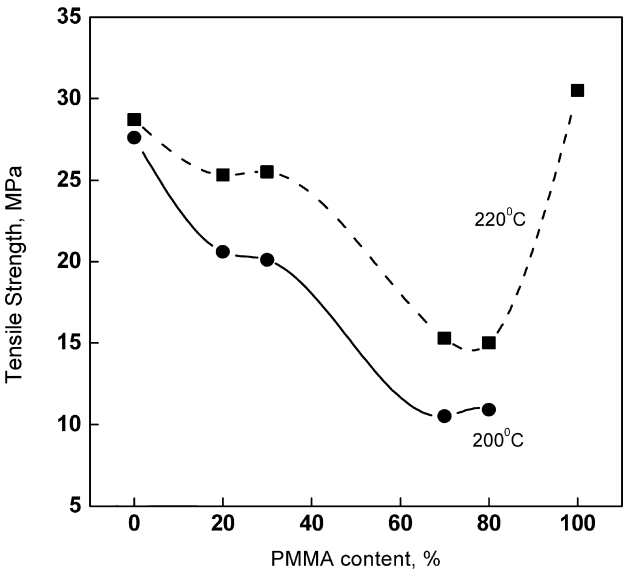

Fig. 5. Effect of PMMA contents on tensile strength of PS/PMMA blends with weld-line.

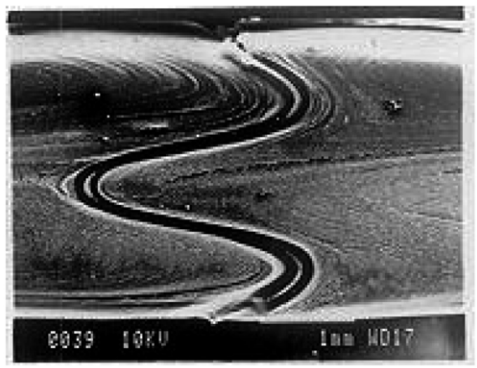

a. longitudinal section, whole weldline

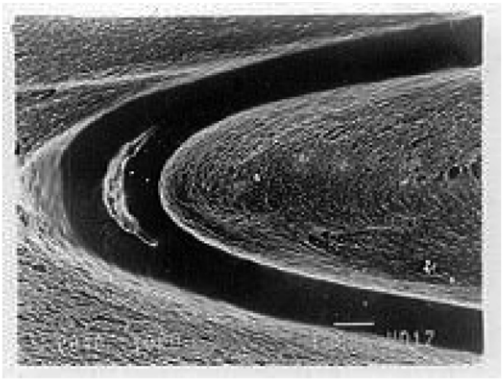

b. longitudinal section, center of weldline

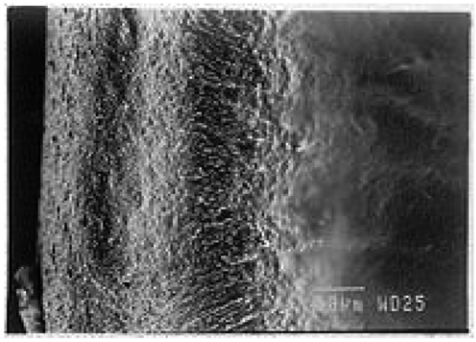

c. cross section, skin

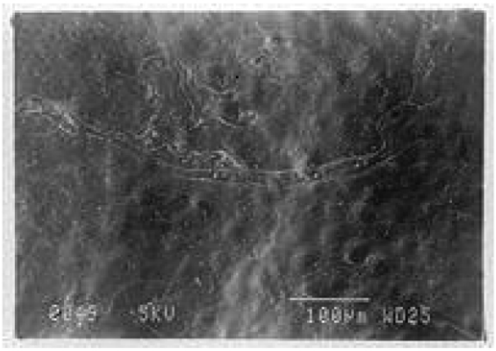

d. cross section, center

Fig. 6. SEM photographs of cross and longitudinal sections of weld-line for PMMA/PS (70/30) (injection temperature: 240 °C).

However, a shiny surface with smooth topography is observed at the center (Fig. 6c and d).

4. Theory

Kim and Suh [8] have developed a model for the prediction of weld-line strength as a function of temperature and contact time for glassy and amorphous polymers. Mekhilef et al., [43] have widen this study to the prediction of weld-line strength as a function of temperature and contact time for immiscible polymer blends. The weld-line strength is proportional to molecular bonding area across the interface. The weld-line strength σ_w may be expressed as

$$\sigma_w = \sigma_b\left(\frac{A_0 - A_N}{A_0}\right) \tag{1}$$

where σ_w and σ_b are the tensile strength of the injection molded part with and without weld-line, respectively, A_0 is the initial cross-sectional area of the interface, A_N is the non-bonded area, and $A_0 - A_N$ is the bonded area at specific contact time.

A_N variation rate with t can be given by Fick's Law:

$$\frac{dA_N}{dt} = C\frac{D\,\Delta G}{kT} \tag{2}$$

where C is a constant, D is diffusion coefficient, and k is the Boltzmann constant, T is the absolute temperature, t is the contact time, ΔG is the free-energy difference, and written as:

$$\Delta G = -2\gamma A_N - T\Delta S_m \tag{3}$$

where γ is the surface tension, and ΔS_m is the entropy of mixing determined from the Flory–Huggins theory of lattice [62].

$$\Delta S_m = -kTA_N\,\delta x\,\delta n_0 \ln(1/2) \tag{7}$$

where δx and δn_0 are the diffusion thickness and the number of lattice per unit volume, respectively.

Combining Eqs. (2)–(7), (dA_N/dt) may be expressed as:

$$\frac{1}{A_N}dA_N = -\frac{CD}{kT}\left(2\gamma - kT\,\delta x\,\delta n_0 \ln(1/2)\right)dt \tag{8}$$

In the model prediction for amorphous polymers proposed by Kim and Suh [8] and the model prediction for immiscible polymer blends proposed by Mekhilef et al., [43], δx is considered as a constant. Hence, integrating Eq. (8), the

model prediction for amorphous polymers is given by [8]:

$$\frac{\sigma_w}{\sigma_b} = 1 - \exp\left\{-\frac{CD}{kT}(-2\gamma + kT\,\delta x\,\delta n_0 \ln(1/2))t\right\} \quad (9)$$

The model prediction for immiscible polymer blends is expressed as [10]:

$$\begin{aligned}\frac{\sigma_w}{\sigma_b} &= 1 - \phi_A^2 \exp\left\{\frac{C_A D_A}{kT}\left(2\gamma_A + kT\,\delta x_A \delta n_A \ln\left(\frac{1}{2}\right)\right)t\right\} \\ &- \phi_B^2 \exp\left\{\frac{C_B D_B}{kT}\left(2\gamma_B + kT\,\delta x_B \delta n_B \ln\left(\frac{1}{2}\right)\right)t\right\} \\ &- \left(1 - \phi_A^2 - \phi_B^2\right)\exp\left\{-\frac{C_{AB} D_{AB}}{kT}\left[\gamma_A + \gamma_B - RT\delta_{AB}\right.\right. \\ &\left.\left.\times\left(\frac{\rho_A}{M_A}\phi_A{}'\ln\phi_A{}' + \frac{\rho_B}{M_B}\phi_B{}'\ln\phi_B{}' + \chi_{AB}\phi_A{}'\phi_B{}'\right)\right]t\right\}\end{aligned} \quad (10)$$

here we consider δx as a function of time, $\delta x = 2(Dt)^{1/2}$, we rewrite the models as follows:

for glassy and amorphous polymers:

$$\frac{\sigma_w}{\sigma_b} = 1 - \exp\left\{-\frac{CD}{kT}\left[2\gamma - \frac{4}{3}kTD^{1/2}\delta n \ln\left(\frac{1}{2}\right)t^{1/2}\right]t\right\} \quad (11)$$

for amorphous polymer blends, the model prediction for weld-line strength is given by:

$$\begin{aligned}\frac{\sigma_w}{\sigma_b} &= 1 - \phi_A^2 \exp\left\{-\frac{C_A D_A}{kT}\left[2\gamma_A - \tfrac{4}{3}kTD_A^{1/2}\delta n_A \ln(1/2)t^{1/2}\right]t\right\} \\ &- \phi_B^2 \exp\left\{-\frac{C_B D_B}{kT}\left[2\gamma_B - \frac{4}{3}kTD_B^{1/2}\delta n_B \ln(1/2)t^{1/2}\right]t\right\} \\ &- (1 - \phi_A^2 - \phi_B^2) \\ &\times \exp\left\{-\frac{C_{AB} D_{AB}}{kT}\left[\gamma_A + \gamma_B - \tfrac{4}{3}RTD_{AB}^{1/2}\delta n_{AB} t^{1/2}\right.\right. \\ &\left.\left.\times\left(\frac{\rho_A}{M_A}\phi_A \ln\phi_A + \frac{\rho_B}{M_B}\phi_B \ln\phi_B + \chi_{AB}\phi_A\phi_B\right)\right]t\right\}\end{aligned} \quad (12)$$

In this work, we will use Eq. (11) for predicting weld-line strength of PS and PMMA, and Eq. (12) for predicting the weld-line strength of PS/PMMA blends.

Self-diffusion can be calculated by following equation [59].

$$D\eta = (A\rho kT/36)R^2/M \quad (13)$$

where A is Avagodro's number, R^2/M is essentially a constant for any bulk polymer. If η is known, it is possible to predict D. The viscosities of PS, PMMA and PS/PMMA are shown in Table 1. The viscosity at other temperatures can be easily calculated by Arrhenius equation. Fox and Allen [60] has reported that the constant R^2/M for PS and PMMA is 4.68×10^{-17} and 3.72×10^{-17}, respectively.

The mutual diffusion coefficient D_{AB} is given by following expression [61]

$$\begin{aligned}D_{AB} &= \phi(1-\phi)\Lambda_0 \frac{N_e}{N} \\ &\times\left(\frac{1}{N\phi} + \frac{1}{N(1-\phi)} + 2|\chi_{AB}|\right)kT\end{aligned} \quad (14)$$

where ϕ is volume fraction of dispersed phase, Λ_0 is the mobility coefficient, N_e is the degree of polymerization for entanglement and N is the degree of polymerization. Usually for $\Lambda_{0A} \neq \Lambda_{0B}$ and $N_A \neq N_B$, the diffusion coefficient is given by

$$D_{AB} = D_0 \frac{\phi(1-\phi)}{\phi + k(1-\phi)} \quad (15)$$

where

$$D_0 = 2|\chi_{AB}|kT\Lambda_{0B}, \qquad k = \frac{\Lambda_{0B}}{\Lambda_{0A}}, \qquad N < N_e \quad (16)$$

$$D_0 = 2|\chi_{AB}|kT\Lambda_{0B}\frac{N_e}{N_B}, \qquad k = \frac{\Lambda_{0B}}{\Lambda_{0A}}\frac{N_A}{N_B}, \quad (17)$$

$N < N_e$

According to Rouse theory [62], the friction ξ can be related to the viscosity:

$$\xi = \frac{1}{\Lambda_0} = \frac{36M_0}{\rho R^2 N_A}\eta_{0cr} \quad (18)$$

where M_0 is molecular mass of a monomer unit, η_{0cr} is a critical viscosity which is given by:

$$\begin{aligned}\eta_{0cr} &= \eta_0\left(\frac{M_{cr}}{M_w}\right)^{3.4} \qquad \text{if } M_w > M_{cr} \\ \eta_{0cr} &= \eta_0\left(\frac{M_{cr}}{M_w}\right) \qquad \text{if } M_w < M_{cr}\end{aligned} \quad (19)$$

where η_0 is zero shear viscosity, M_{cr} is a critical molecular weight. $M_{cr} = 2M_e$, $M_e = \rho RT/G^0$, G^0 is the plateau modulus. η_0 and G^0 can be measured by oscillatory rheometer. η_0 is listed in Table 1. In literature [63], G^0 is equal to 4.5×10^6 dyne/cm^2 for PMMA, 180 °C, and 2.0×10^6 dyne/cm^2 for PS, 190 °C. In our measurement, G^0 is taken G' corresponding to when tan δ is minimum at plateau region [64], G^0 is equal to 1.7×10^5 N/m^2 for PS, 180 °C, and 4.45×10^5 N/m^2 for PMMA, 180 °C which coincides with that reported in literature. Introducing the friction coefficients in the diffusion equation, we can calculate D_{AB}.

The surface tension from literature is listed in Table 2 [64].

5. Model predictions

Figs. 7 and 8 show the prediction of the weld-line strength as a function of contact time at different melt

Table 2
Surface tension (mN/m) of PMMA and PS

Sample	γ (mN/m)			$-d\gamma/dT$ (mN/m °C)
	20 °C	150 °C	200 °C	
PS	40.7	31.4	27.8	0.072
PMMA	42.7	31.0	26.5	0.090

temperatures for pure PS and PMMA, respectively. The bonding area at the weld-line increases with the increase of contact time and temperature. The total bonding can be achieved at 280 and 300 °C within 10 s for PS and PMMA, respectively. However, when the melt temperature drops close the glass temperature, incomplete bonding is occurred. Since the diffusion of molecular chains at temperature close glass temperature of the materials is weaken. For polymer blends, the bonding area at the interface of PS/PMMA (80/20, 70/30, 20/80) increases with the rise of contact time and melt temperature (Fig. 9). However, the bonding area for PS/PMMA blends (80/20 and 70/30) increases faster with contact time and temperature than for PMMA/PS blends for PMMA matrix does. In this temperature range $T > 160$ °C, both phases contribute to the adhesion of the melt fronts. This slow increase is also awarded to the variation of the diffusion coefficient D of PMMA and D_{AB} for PMMA matrix blend are lower than D of PS, and D_{AB} for PS matrix blend, respectively.

5.1. Validation of the model prediction

As shown in Figs.10 and 11, for PS, PMMA, PS/PMMA (80/20), PS/PMMA (70/30), the predicted σ_w/σ_b is found in good agreement with experimental results. However, for PMMA/PS (80/20), PMMA/PS (70/30), the predicted σ_w/σ_b is much higher than the experimental results. Since, in our model for polymer blends, we consider three kinds of diffusion: PMMA-PMMA, PS-PS, PMMA-PS which all contribute to weld-line strength. But in fact, there is only one kind of diffusion, matrix PMMA self-diffusion for PMMA/PS (80/20, 70/30). The dispersed PS phase highly oriented along the weld-line inhibits the diffusion of PMMA on weld-line. Then, we can conclude that the weld-line strength for amorphous homopolymers and their blends, and where the viscosity of the matrix lower than that of dispersed phase, can be modeled by Fick's diffusion Law. However, the use of the model taking into account just the coefficient diffusion, as well as the operating parameters, e.g. melt temperature and contact time overestimate the orientation and size of dispersed phase at weld-line. The weld-line strength is not only attributed to diffusion phenomenon, as well the bonding area. Therefore, it is important to consider the orientation effect at weld-line.

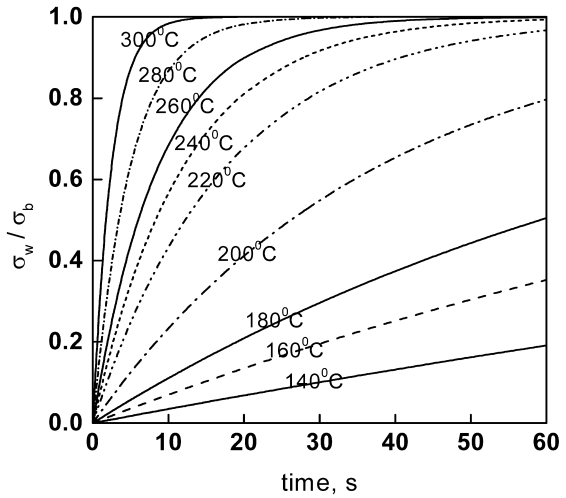

Fig. 8. Model predictions for weld-line strength of PMMA as a function of temperature and contact time.

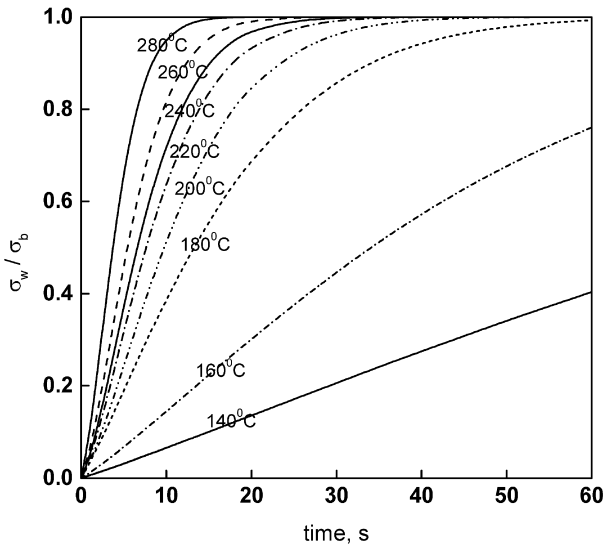

Fig. 7. Model predictions for weld-line strength of PS as a function of temperature and contact time.

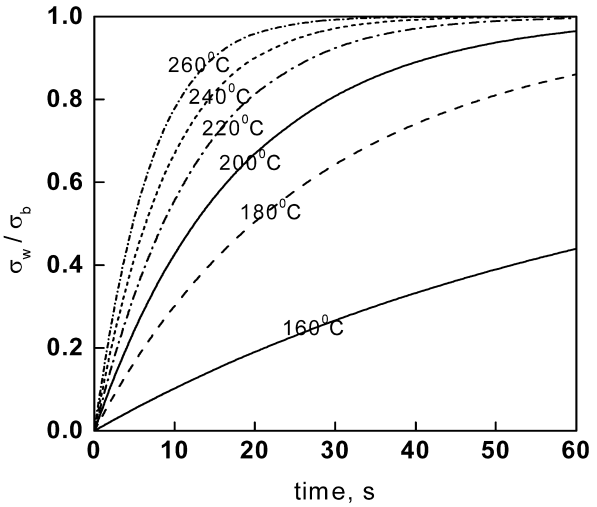

Fig. 9. Model predictions for weld-line strength of PS/PMMA (80/20) as a function of temperature and contact time.

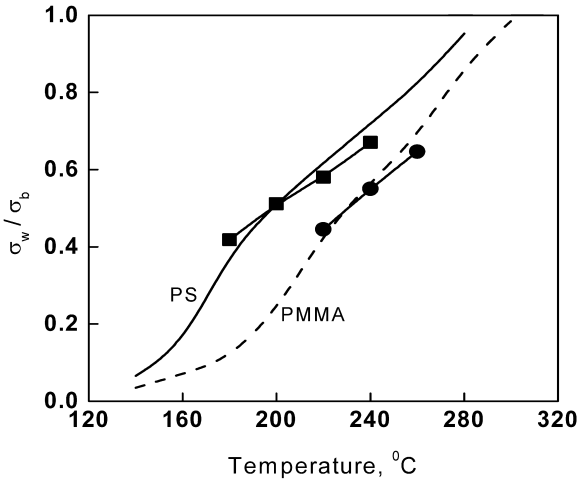

Fig. 10. Comparison of model predictions for weld-line strength of PS and PMMA with their corresponding experimental data.

This might that for PMMA/PS blend, the predicted σ_w/σ_b goes away from experimental results (Fig. 11).

6. Conclusions

A model based on Flory–Huggins lattice theory and Fick's law for predicting the weld-line strength of injection molded polymer parts has been modified by introducing diffusion thickness as a function of temperature and contact time. The modified model has been used to predict the weld-line strength of injection molded parts for PS, PMMA and their blends as a function of injection temperature and contact time. The model predictions for amorphous PS and PMMA are in good agreement with the experimental results. For PS/PMMA blends, (PS is matrix), the model predictions for PS/PMMA (80/20), PS/PMMA (70/30) match with experimental data. However, the model does not take into account the orientation difference and the absence of dispersed phase in the weld-line region. The tensile strength of injection molded PS/PMMA-WL blends decreases, while the tensile strength without weld-line increases with the increase of the PMMA content.

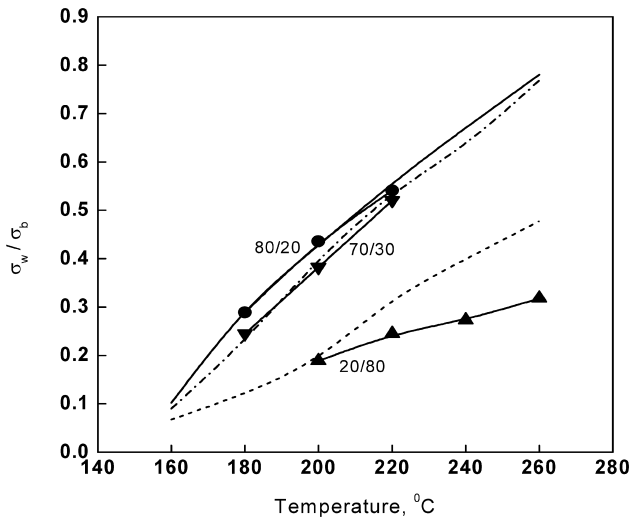

Fig. 11. Comparison of model prediction for weld-line strength of PS/PMMA (80/20, 70/30, 20/80) blends with experimental data.

Acknowledgements

The authors are grateful to the Special Funds for Major State Basic Research Projects of China (G1999064800), National Natural Science Foundation of China (20174025, 20274029) and the State Education Ministry of China for financial support of this work.

References

[1] Fellahi S, Meddad A, Fisa B, Favis BD. Adv Polym Technol 1995; 14(3):169.
[2] Bozarth MJ, Hamill JL. SPE ANTEC Tech Papers 1984;30:1091.
[3] Bangert H. Kunstst Ger Plast 1985;75:15.
[4] Tomari K, Harada T. Polym Engng Sci 1993;33(15):996.
[5] Hagerman EM. Polym Engng 1993;29:67.
[6] Kim JK, Song JH, Chung ST, Kwon TH. Polym Engng Sci 1997; 37(1):228.
[7] Hobbs SY. Polym Engng 1974;14:621.
[8] Kim SG, Suh NP. Polym Engng Sci 1986;26(17):1200.
[9] Tomari K, Tonogai S, Harada T, Hamada H, Lee K, Morii T, Maekawa Z. Polym Engng Sci 1990;30:931.
[10] Malguarnera SC. Polym Plast Tech Engng 1982;18:1.
[11] Malguarnera SC, Manisali AT, Riggs DC. Polym Engng Sci 1981;25: 1149.
[12] Selden R. Polym Engng Sci 1997;37(1):205.
[13] Singh D, Mosle HG. Makromol Chem. Macromol Symp 1988;20/21: 489.
[14] Mosle HG, Criens RM, Dirk H. SPE ANTEC Tech Papers 1984;30: 772.
[15] Piccarolo S, Salu M. Plast Rubber Process Appl 1988;10:11.
[16] Janickl SL, Peter RP. SPE ANTEC Tech Papers 1991;37:391.
[17] Gardner G, Cross C. SPE ANTEC Tech Paper 1992;38:2127.
[18] Malguarnera SC, Manisali AI, Riggs DC. Polym Engng Sci 1981;21: 17.
[19] Titomanlio G, Piccarolo S, Rallis A. Polym Engng Sci 1989;29:4.
[20] Kim S, Suh NP. Polym Engng Sci 1986;26:17.
[21] Ulcer Y, Cakmak M, Hsiung CM. J Appl Polym Sci 1995;55.
[22] Fisa B, Rahmani M. Polym Engng Sci 1991;31:18.
[23] Poue BK. SPE ANTEC Tech Paper 1995;495.
[24] Malloy R, Gardner G, Grossman E. SPE ANTEC Tech Paper 1993; 521.
[25] Piccarolo S, Scargiali F, Crippa G, Titomanlio G. Plast, Rubber Compos Process Appl 1993;19(4):205.
[26] Wang L, Allen PS, Bevis MJ. Plast, Rubber Compos Process Appl 1995;23(3):139.
[27] Tjader T, Seppala J, Jaaskelainen P. J Mater Sci 1998;33:923.
[28] Wenig W, Stolzenberger C. J Mater Sci 1996;31:2487.
[29] Criens RM, Mosle HG. In: Brostow W, Corneliussen RD, editors. Failure of plastics. Munich: Hanser; 1986.
[30] Wenig C. Kunstst Ger Plast 1992;82:3.
[31] Piccarolo S, Rallis A, Titomanlio G. Plast Rubber Process Appl 1987; 10:11.
[32] Gilmore GD, Spencer RS. Mod Plast 1951;28(8):117.
[33] Bucknall CB. Pure Appl Chem 1986;58:985.

[34] Kamel MR, Moy FH. J Appl Polym Sci 1983;28:1787.
[35] Katti SS, Schultz JM. Polym Engng Sci 1980;22:197.
[36] Singh D, Mosle HG, Kunz M, Wenig W. J Mater Sci 1990;25:4704.
[37] Wenig W, Singh D, Mosle HG. Angew Makromol Chem 1990;179: 35.
[38] Singh D, Mosle HG. Makromol Chem Macrom Symp 1988;20/21: 489.
[39] Bell RG, Cook CD. Plast Engng 1979;8:18.
[40] Wendt U. Kunstst Ger Plast 1988;78:123.
[41] Mielewski DF, Bauer DR, Schmitz PJ, Van Oene H. Polym Engng Sci 1998;38(12):2020.
[42] Nolley E, Barlow JW, Paul DR. Polym Engng Sci 1980;20:364.
[43] Mekhilef N, Ait-Kadi A, Ajji A. Polymer 1995;36(10):2033.
[44] Brahimi B, Ait-Kadi A, Ajji A. Polym Engng Sci 1994;34(15):1202.
[45] Thamm RC. Rubber Chem Tech 1977;50:24.
[46] Malguarnera SC, Riggs DC. Polym Plast Tech Engng 1981;17:193.
[47] Karger-Kocsis J, Csikai I. Polym Engng Sci 1987;27:241.
[48] Fisa B, Favis BD, Bourgeois S. Polym Engng Sci 1990;30(17):1051.
[49] Fellahi S, Favis BD, Fisa B. Polymer 1996;37(13):2615.
[50] Nadkarni VM, Ayodhya SR. Polym Engng Sci 1993;33(6):358.
[51] Fellahi S, Fisa B, Favis BD. J Appl Polym Sci 1995;57:1319.
[52] Worden E, Kushion S. SPE ANTEC Tech Papers 1991;37:2653.
[53] Pecorini J, Seo KS. Plast Engng 1996;52(5):31.
[54] Hamada H, Tomari K, Yamane H, Senba T, Hiragushi M. SPE ANTEC Tech Papers 1997;1:1071.
[55] Fisa B. In: Mallick PK, Newman S, editors. Composite materials technology: processes and properties. Munich: Hanser; 1990.
[56] Kamel MR, Tan V. Polym Engng Sci 1979;19:558.
[57] Criens RM, Mosle HC. Polym Engng Sci 1983;23:591.
[58] Mekhilef N, Verhoogt H. Polymer 1996;37(6):4069.
[59] Bueche F, Cashin WM, Debye P. J Chem Phys 1952;20(12):1956.
[60] Fox TG, Allen VR. J Chem Phys 1964;41(2):344.
[61] Brochard F, Jouffroy J, Levinson P. Macromolecules 1983;16:1638.
[62] Flory PJ. Principles of polymer chemistry. Ithaca, NY: Cornell University Press; 1978.
[63] Wu S. J Polym Sci-Phys 1989;27:723.
[64] Wu S. J Polym Sci-Phys 1987;25:557.